Induced Orientation of α-Helical Polypeptides in Polyelectrolyte Multilayers†

M. Müller,* B. Kessler, and K. Lunkwitz

Institute of Polymer Research, Dresden e.V., Hohe Strasse 6, D-01069 Dresden, Germany

Received: December 23, 2002; In Final Form: May 8, 2003

Polyelectrolyte multilayers (PEMs) consisting of stiff polypeptides at texturized silicon substrates were studied. These studies are focused on anisotropic PEMs in contrast with common ones consisting of flexible polyelectrolytes. When stiff polycation poly(L-lysine hydrobromide) (PLL, $M_w = 200000$ g/mol) was used at pH = 11 or in the presence of $NaClO_4$, a transition from random coil (R−PLL) to α-helix (α-PLL) was found. When stiff polyanion poly(L-glutamic acid) (PLG, $M_w = 70000$) was chosen, the α-helical conformation (α-PLG) was adopted at pH = 3. The conformation was checked by IR spectroscopy and circular dichroism. The layer-by-layer technique was used in order to get homogeneous thin films of the polypeptides. Texturized Si-ATR-substrates with parallel nanosized grooves 50−70 nm in width were used for orienting the α-helical polypeptides with contour length $L > 70$ nm. Two different types of PEMs were fabricated: (i) α-PLG/poly(diallyldimethylammoniumchloride) (PDADMAC) and (ii) α-PLL/poly(vinyl sulfate) (PVS). The orientation was studied by dichroic ATR-FTIR spectroscopy using polarized light. An ATR-FTIR-dichroism concept was applied, which was established at low molecular liquid-crystalline systems. Via the dichroic ratio of the amide I and II band areas measured with parallel (A_p) and with vertically polarized IR light (A_s) an order parameter S could be determined, knowing the angle θ between the α-helical axis and the amide mode transition dipole moments. S is a measure for the uniaxial orientation of the multilayer embedded polypeptides within the nanogrooves of the silicon plate, where $S = 0$ means no and $S = 1$ means high orientation. $S > 0.5$ was found for both multilayer embedded α-PLL and α-PLG (i and ii), indicating a significant orientation with respect to the nanogroove direction. The influence of M_w, concentration, number of adsorption steps, and drying was investigated. PEMs exposing charged α-helical polypeptides in the outermost layer can be used to create biomimetic and biosensor surfaces.

Introduction

Wet chemical surface modification by polyelectrolytes (PELs) is a common processing step in applications such as colloid stabilization and flocculation for water treatment and papermaking. Currently, polyelectrolyte layers are under way to address novel application fields in nano- and bioscience, especially in sensor and biomaterial development. Since by adsorption from single-component solutions often only incomplete monolayers are formed, mixed systems consisting of polycations and polyanions are progressively used in these applications. About 10 years ago the concept of polyelectrolyte multilayers (PEMs), which makes use of the consecutive adsorption of oppositely charged polyelectrolytes, was introduced by Decher[1,2] to create coatings of defined and controlled thickness on various kinds of surfaces. Whereas the early work on PEMs was both inspired and aimed at defined nanoscopic layered structures of extended polyelectrolytes, it is now commonly accepted that the multilayer phase is more or less isotropic ('fuzzy').[2] This picture was experimentally proved by the absence of Bragg peaks obtained by both X-ray reflectivity, e.g., refs 3 and 4, and small angle neutron reflectivity, e.g., refs 2 and 5, studies on PEMs of charged flexible PELs. Currently, the internal structure of PEMs is claimed to be similar to the core zone of dispersed polyelectrolyte complexes (PECs), prepared by directly mixing polycation and polyanion solutions, which was theoretically described by Borue[6] and Joanny[7] to be composed of entangled Gaussian coils (random phase approximation).

Nevertheless, there are exceptions from those isotropic PEMs. Recently, Laschewsky reported lamellar nanostructures in PEMs composed of lyotropic ionenes and strong polyanions which could be additionally correlated with the internal structure of PECs of the same components.[8] Further concepts for anisotropic PEMs were initiated by Kleinfeld and Ferguson using exfoliated sheets of sheet silicate minerals such as Laponite consecutively adsorbed with polycations.[9] In that framework our approach to anisotropic structures are surface-induced oriented PEMs consisting of polypeptides in their α-helical conformation. This was initially shown for α-helical poly(L-lysine) (PLL) in combination with several polyanions, both in the presence of $NaClO_4$ by dichroic ATR-FTIR spectroscopy.[10]

Experimental Section

Surface. As substrates, trapezoidal internal reflection elements (IRE) of Si ($n_1 = 3.5$, 20 mm wide × 2 mm thick, upper and lower lengths 48 and 52 mm, respectively) with a 45° aperture were used after plasma cleaning (plasma chamber PDC-32G, Harrick (distributed by Starna, Pfungstadt), 1 Torr, 2 min, 100W). IREs were texturized by polishing in the direction of the short (20 mm) edge using a 0.2 μm diamond paste (Markon, Lotzwil, Switzerland), resulting in parallel textures on the SiO surface as described therein.[10] From atomic force (AFM) and scanning electron microscopy (SEM) measurements a mean groove width of about 50−70 nm was found, which is small

† Part of the special issue "International Symposium on Polyelectrolytes".

* To whom correspondence should be addressed. Phone: 0049-351-4658 405. Fax: 0049-351-4658 284. E-mail: mamuller@ipfdd.de.

10.1021/jp027812x CCC: $25.00
Published on Web 07/09/2003

compared to mid-IR wavelengths of 2.5−10 μm. An AFM micrograph and a surface profile of the scratched Si−IRE surface is shown in Figure 4a, b.

Polyelectrolyte Multilayers (PEMs). Solutions of the polypeptides poly(L-lysine) (PLL, Sigma, $M_w = 20000$, 200000, 300000 g/mol) and poly(L-glutamic acid) (PLG, $M_w = 70000$ g/mol) were brought to pH = 11 and 3 by titrating with NaOH or HCl, respectively. As oppositely charged PEL for PLL poly(vinyl sulfate) (PVS, Serva, $M_w = 160000$ g/mol) and for PLG PDADMAC ($M_w = 2500000$, 9000 g/mol) were used, respectively. Millipore water (18.2 MΩ) was used, and the concentrations of the solutions ranged from 0.01 to 0.001 M. Multilayers of oppositely charged polyelectrolytes (PEMs) were fabricated on the Si−IRE surfaces in the sample compartment of the ATR−IR sorption cell (IPF Dresden) by consecutive adsorption/rinsing cycles, according to the stream-coating procedure described therein[11] using syringes or an automated dosage system. The PEMs were dried by a gentle N_2 stream above the Si−IRE in the sample compartment. PEM-5 resulted in brownish films of around 50−100 nm (empirical determination).

ATR-FTIR Spectroscopy. The in-situ ATR-FTIR apparatus for sorption measurements (U. P. Fringeli, University of Vienna, OPTISPEC, Zürich),[12] consisting of a special mirror setup and the in-situ sorption cell (IPF Dresden), was used on a commercial rapid scan FTIR spectrometer (IFS 28, BRUKER) equipped with a globar source and MCT detector, as described elsewhere. ATR-FTIR absorbance spectra were recorded by the SBSR (single-beam sample reference) method,[12] whereby single-channel spectra $I_{S,R}$ were recorded of both the upper (S) and lower (R) half of the Si−IRE ($50 \times 20 \times 2$ mm^3) by one IR beam. Two liquid chambers (S, R), which are filled with polyelectrolyte solution (S chamber) and water (R chamber), are mounted above the sample and reference half, respectively. Normalizing the single-channel spectra according to $A_{SBSR} = -\log(I_S/I_R)$ resulted in absorbance spectra (A_{SBSR}) with proper compensation of the background absorptions due to the SiO_x layer, the solvent (water), the water vapor (spectrometer), and ice on the MCT detector window.

For the determination of the integrated areas and peak intensities of the ν(CH) (3000−2800 cm^{-1}), the amide A (3450−3250 cm^{-1}), amide I (1680−1610 cm^{-1}, 80% ν(C═O)), and amide II (1590−1480 cm^{-1}, 60% δ(NH)) tight baselines and the integration limits given in brackets, respectively, were used (OPUS software package, BRUKER). Relative errors of 5−10% of the determined areas and peaks led to absolute errors $\Delta S \approx 0.1$ for the order parameters S and of $\Delta\gamma \approx 4°-8°$ for the opening angles γ according to the cone model (computation see below).

For thicknesses up to 100 nm, the electric field components E_x, E_y, and E_z used to calculate the order parameter S are approximately constant, so that the S values of the reported PEMs can be directly compared (see theory).

CD Spectroscopy. A JASCO spectral polarimeter (J-810, JASCO, Gross-Umstadt) was used. CD spectra of the polypeptides PLG and PLL were recorded in the spectral range from 180 to 250 nm. The CD spectra were qualitatively analyzed due to the appearance of the negative 222/208 nm doublet (n−π*, $\pi-\pi$* transitions, respectively) indicative of the α-helical conformation.

Orientation Analysis Using Dichroic ATR-FTIR Data

In-situ ATR-FTIR spectroscopy enables determination of orientation in thin polymer films in the dry state and in contact to the solvent using the dichroism of diagnostic IR bands. Polymer orientation can occur at the molecular, microscopic, and macroscopic level, whereby from the molecular orientation the macroscopic orientation cannot necessarily be inferred. Orientation in polymer systems can be achieved by self organization or by mechanical stretching of polymer films or foils. The degree of orientation can be studied either by transmission-IR spectroscopy, especially at polymer foils, or by ATR−IR spectroscopy predominantly at the surface or in the layer phase of thin supported polymer films. A detailed theoretical treatment of internal reflection spectroscopy is given therein.[12] The principle is demonstrated in Figure 1, whereby the oriented sample on the ATR crystal interacts with p- and s-polarized IR light and the absorbance spectra for each polarization are recorded. s-Polarized light causes exclusively the E_y component of the evanescent electrical field E penetrating from the surface in the adjacent optically thinner medium, whereas p-polarized light results in a linear combination of the E_x and E_z component according to

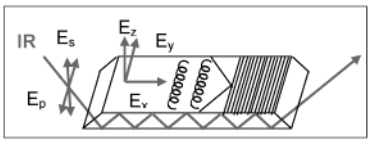

Figure 1. Principle and experimental system of ATR-FTIR dichroism measurements on oriented polymer films in the substrate plane.

$$E_s = E_y \tag{1}$$

$$E_p = (E_x^2 + E_z^2)^{1/2} \tag{2}$$

IR bands of the oriented polymers, whose transition dipole moments M ($M_{x,y,z}$) are situated in the plane of the E_x and E_z components, absorb more p-polarized light, whereas those situated in the E_y direction of the substrate plane absorb more s-polarized light according to

$$\begin{aligned} A &= |E|^2|M|^2 \cos^2(E,M) \\ &= (E_x M_x + E_y M_y + E_z M_z)^2 \end{aligned} \tag{3}$$

The ratio of the integrated areas of the bands measured by p- and s-polarized light A_p and A_s is the dichroic ratio

$$R = A_p/A_s \tag{4}$$

Polymer orientation can occur both vertical or parallel with respect to the surface plane of substrates. Examples for systems with vertical orientation are lipid bilayers[13] or monolayers of surfactant-like molecules[14,15] on planar substrates. In contrast, in that work the parallel or 'in-plane orientation' of charged polypeptides is treated.

The quantitative analysis of ATR-IR dichroic data on *in-plane* oriented organic material was developed by Fringeli for low molecular weight liquid crystalline compounds[16,17] using the formalism of transmission-IR dichroism, which was described by Zbinden.[18] The dichroic ratios measured by ATR-IR spectroscopy have to be corrected first considering the electrical field components. Then further treatment is completely based on transmission IR dichroism. The relevant equations used for analysis of the ATR-IR dichroic data in that report are given in the following equations

$$R_y^{ATR} = \frac{A_p}{A_s} \tag{5}$$

$$R^{T} = R_y^{ATR} \cdot \frac{E_y^{\,2}}{(E_x^{\,2} + E_z^{\,2})} \tag{6}$$

$$S = \frac{(1 - R^{T})}{(2R^{T} + 1)} \cdot \frac{2}{(3\cos^2\theta - 1)} \tag{7}$$

$$\gamma = \arccos\left(\sqrt{\frac{2}{3}S + \frac{1}{3}}\right) \tag{8}$$

In the first step of the analysis the dichroic ratio has to be determined by dividing the integrated area or peak height of an IR band of the p-polarized and that of the s-polarized spectrum according to eq 5. Further, via eq 6 the dichroic ratios of ATR-IR spectroscopy, the R_y^{ATR} values, are transformed into dichroic ratios R^T of IR transmission spectroscopy knowing the relative electric field components $E_{x,y,z}$. This R^T value is then compatible with the dichroic ratio used in common spectroscopic orientation theories. We followed a methodical concept which was initially applied on low molecular weight liquid crystals[16] under slight variation of the algebra. Using eq 7 and knowing the angle θ between the transition dipole moment of the amide I and amide II bands with respect to the molecular (α-helical) axis of polypeptides, an order parameter S can be determined. The order parameter determined by eq 7 is identical with the orientation function f introduced by Hermanns,[19] which is commonly used in polymer spectroscopy. f is the mean second Legendre polynom $f = \langle P_2(\cos\theta)\rangle = (3\langle\cos^2\theta\rangle - 1)/2$.[20] Furthermore, by eq 8 the opening angle γ of a double cone can be determined, which can be used as a distribution model of a more or less aligned bundle of polymer rods (see Figure 11a). The cone opening angle $\gamma = 0°$ for high and $\gamma = 54.5°$ for low order or low degree of uniaxiality. In Figure 2 the relative positions of the transition moments of the amide I and II bands with respect to the molecular (helical) axis are shown. The angles $\theta = 38°$ (amide I) and $\theta = 73°$ (amide II) were taken from the theoretical results of Miyazawa[21] and Krimm,[22] which were confirmed recently by Marsh.[23] In Figure 3 the dependence of the order parameter S on the dichroic ratio R^T is shown for both amide bands taking the thin film approximation[12,17] and dry state of the sample into account for the evaluation of the electric field components ($E_{x,y,z}$) of eqs 1, 2, 3, and 6. Evidently, high order parameters S are reached in the case of dichroic ratios $R^T < 1$ for the amide I band and $R^T \gg 1$ for the amide II band. Bands with $R^T < 1$ may be called 'parallel', and those with $R^T \gg 1$ may be called 'vertical' (with respect to the molecular axis and for that specific system with textures in the E_y direction), which is evident from Figure 2. For both amide bands the order parameter $S = 0$ in the case of $R^T = 1$ under the assumption of planar polymer orientation. An order parameter $S = -0.5$ is obtained if a band erroneously assumed as 'parallel' shows $R^T \gg 1$ and therefore has to be corrected as 'vertical' and if a band erroneously assumed as 'vertical' shows $R^T \ll 1$ and therefore has to be corrected as 'parallel'. This can be used analytically for that specific system (E_y in groove direction), so that bands can be approximately classified in parallel or vertical ones.

This concept was first applied on thin films of α-helical poly(γ-methylglutamate-*co*-γ-octadecylglutamate) (PMOLG), introduced as hairy rod-like molecules by Wegner,[24] which was reported therein.[25] Using the same data the orientation analysis was refined by Marsh[23] with respect to further amide modes. Whereas these oriented α-helical polypeptide films were inherently hydrophobic in that paper, we report on oriented multilayer films of the hydrophilic α-helical polypeptides poly(L-lysine) (PLL) and poly(L-glutamic acid) PLG.

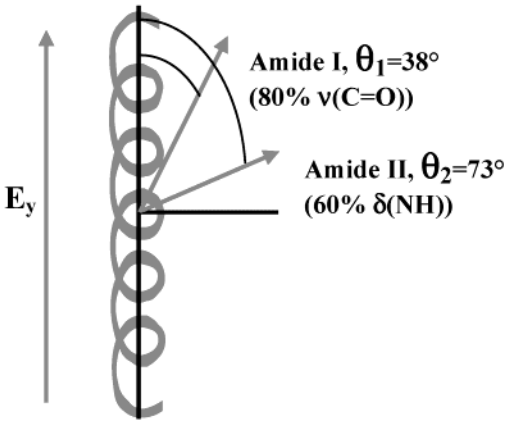

Figure 2. Directions of the transition dipole moments of the amide I and amide II vibrations relative to the α-helical axis.

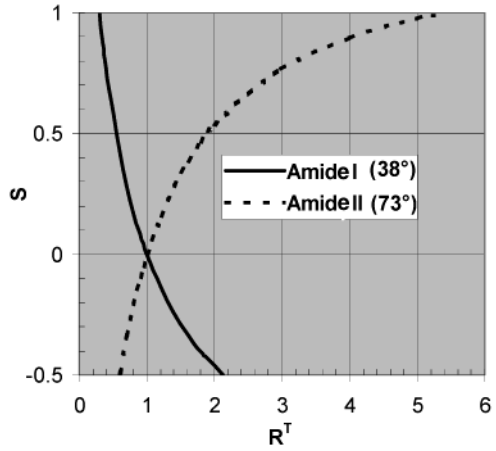

Figure 3. Dependence of the order parameter S on the dichroic ratio R^T for the amide-I (parallel) and amide-II band (vertical).

Results

In the following, results on the orientation of the charged polypeptides PLL and PLG within PEMs are shown. PLL and PLG are known to adopt various conformations in the solution and at the surface by variation of external parameters such as the pH, ionic strength and type, solvent, and temperature.[26−29] Two systems, one with the anionic polypeptide PLG combined with the strong polycation PDADMAC and one with the cationic polypeptide PLL and the strong polyanion PVS, were chosen as model systems. In that report the α-helix of PLG and PLL was predominantly induced by pH. Consequently, we used strong oppositely charged polyelectrolytes whose charge density is not dependent on the pH. This had the advantage that the aqueous media of pH = 3 and 11 for keeping the α-helix of PLG as well as the α-helix of PLL, respectively, did not change the charge state of PDADMAC and PVS, respectively.

Substrates. The idea was to grow oriented multilayers of polypeptide rods complexed with oppositely charged PELs on a command substrate, which was texturized by parallel surface grooves. An AFM image of the substrate used is given in Figure 4a showing parallel textures on the surface.

The formed surface grooves had widths of ≈50−70 nm and heights ≈5−8 nm. This groove size should be sufficiently small

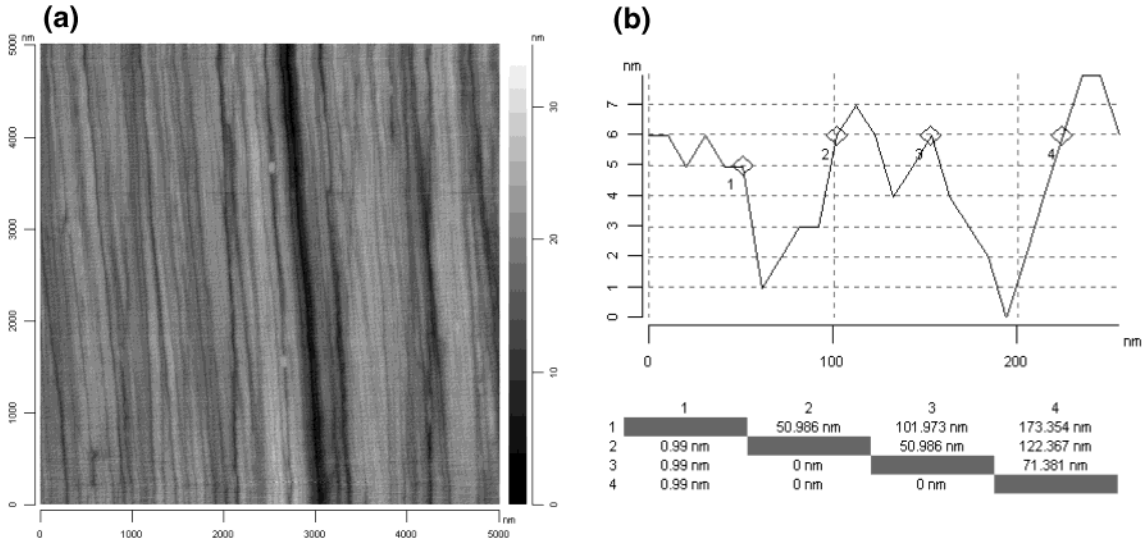

Figure 4. (a) AFM image of the texturized Si−IRE. (b) Surface profile of the texturized Si−IRE, shown in Figure 4a.

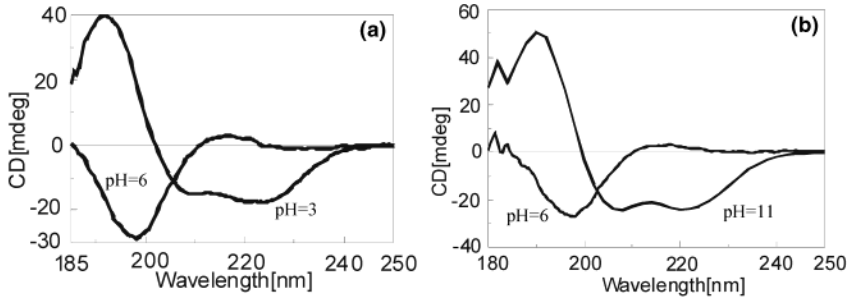

Figure 5. (a) CD spectra of PLG solutions at pH = 6 and 3 (c = 0.001 M, H_2O). (b) CD spectra of PLL solutions at pH = 6 and 11 (c = 0.001 M, H_2O).

to induce a parallel alignment of stiff polymers such as the α-helical polypeptides.

Polypeptide Conformation. In previous studies, perchlorate anions were used to induce the α-helical conformation of PLL within multilayers,[10] which was first described in ref 30. Additionally, it was also reported that PLL adopts the α-helical conformation at pH = 11,[26] where the polypeptide is uncharged. On the other hand, no specific conformation influencing small cations is known to induce the α-helix of the PLG. Since this polypeptide also adopts the α-helical conformation at pH = 3, generally the pH was used as a conformation-inducing parameter for both polypeptides. This was checked by circular dichroism on 0.001 M solutions. CD spectra of PLG at pH = 6 and 3 are shown in Figure 5a.

Significantly, the negative doublet at 208/222 nm (n−π*/π−π* transition of C═O group) shows the α-helical conformation of PLG at pH = 3. However, the negative CD absorption at 190 nm can be assigned to the random coil conformation of PLG at pH = 6. Obviously, the α-helix is stable in the uncharged state, whereas the charged state induced the random coil structure of the polypeptide. Similar spectra are given in Figure 5b for PLL at pH = 6 and 11, whereby again the charged groups (pH = 6) induced the coil conformation. If we assume a perfect α-helix of these polypeptides, given the degree of polymerization N = 1000 for PLL (M_w = 200000 g/mol) and N = 500 for PLG (M_w = 70000), rod lengths (contour lengths) of $L \approx$ 150 and 75 nm can be determined, respectively. PLL and PLG solutions were kept at these pH values for the consecutive multilayer deposition.

α-PLG/PDADMAC at pH = 3. First we present data on PEMs consisting of the anionic α-helical poly(glutamic acid) (PLG) and of PDADMAC (M_w = 250000 g/mol). Since the Si substrate has a negative surface charge, PDADMAC was adsorbed in the first (PEM-1) and further odd adsorption steps and PLG was adsorbed in the second (PEM-2) and further even adsorption steps. Both solutions were brought to pH = 3 in order to keep the α-helical conformation of PLG also in the PDADMAC steps. The consecutive deposition of PDADMAC and PLG from PEM-1 to PEM-6 was monitored by ATR-FTIR spectroscopy. Figure 6a shows a continuously increasing intensity of the respective absorbance spectra. An intense IR spectrum of the PEM was already obtained after the second adsorption step, whereby PDADMAC had only a minor contribution to the spectrum. The diagnostic amide I and II

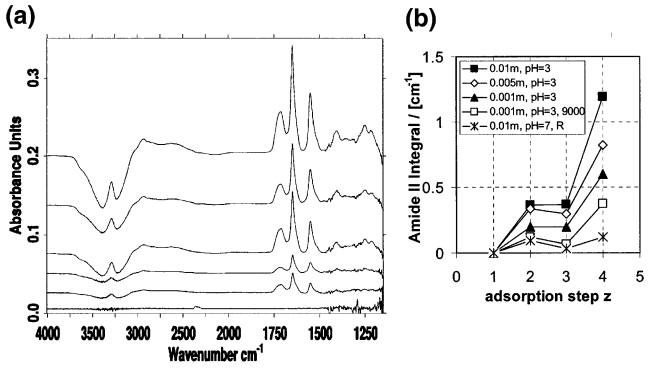

Figure 6. (a) In-situ-ATR-FTIR spectra on the consecutive adsorption of PDADMAC and PLG (from bottom to top, PEM-1 to PEM-6) on the Si−IRE at c = 0.01 M, pH = 3. (b) Integrated areas of the amide I band from the ATR-FTIR spectra of PEM-1 to PEM-4 of PDADMAC/PLG at different pHs, concentrations (0.01−0.001 M), and M_w.

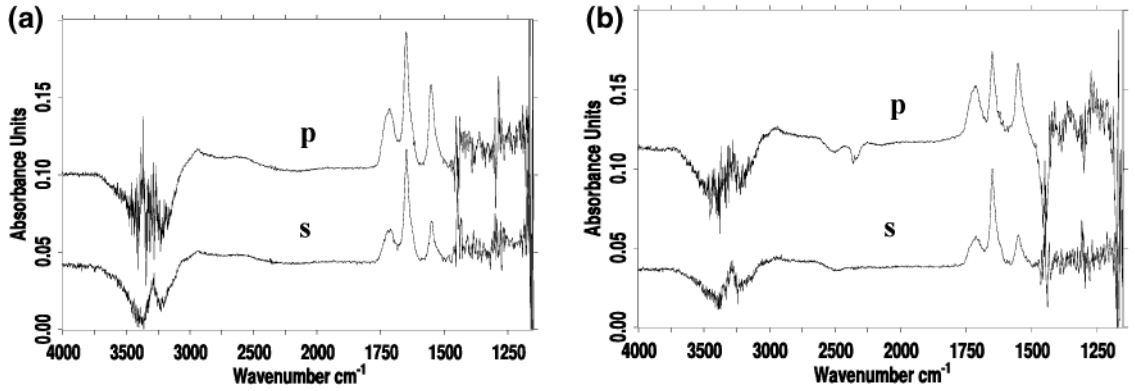

Figure 7. (a) p- and s-polarized ATR-FTIR-spectra of the PEM-4 of PDADMAC/PLG on the untexturized Si−IRE in contact with water (wet) at pH = 3. (PDADMAC, 9000 g/mol; PLG, 70000 g/mol). (b) p- and s-polarized ATR-FTIR-spectra of the PEM-4 of PDADMAC/PLG on the texturized Si−IRE in contact with water (wet) at pH = 3. (Both spectra were scaled by ×3.)

bands of the multilayer embedded PLG appeared at 1650 and 1550 cm^{-1}, which can be unambiguously assigned to the α-helical conformation of PLG.[31] Obviously this correlated with the CD spectra of Figure 5a due to the solution state of PLG.

The increasing integrated areas of the amide II band from Figure 6a can be used as a semiquantitative measure for multilayer growth, as described in ref 32. Hence, the influence of various parameters such as concentration, pH, and M_w of PDADMAC (250000 vs 9000 g/mol) on the adsorbed amount can be studied, which is shown in Figure 6b. The highest adsorbed amount was obtained for the highest concentration. The lowest adsorption was obtained at pH = 7, where PLG adopted the random conformation. It is possible that in that conformation the charged COO^--groups were not exposed at outer spheres in comparison to the PLG α-helix, where the side chains with the COOH groups are directed away from the spectra helical axis[33] and might be better accessible for the PDADMAC.

However, in the spectra of Figure 6a, the ν(C═O) band around 1700 cm^{-1} due to the COOH groups is still present in the PDADMAC steps. Hence, presumably at pH = 3 some cationic groups of PDADMAC were able to displace the protons of the COOH groups of PLG forming ion pairs, but the majority of the COOH groups remained undissociated, which would point more to a nonelectrostatic contribution in PEMs of PDADMAC/PLG.

The higher adsorption level at pH = 3 might also be caused by the higher salt (HCl) content of the PDADMAC and PLG solutions causing a higher coiling of PDADMAC. A low level of adsorption was also obtained for PEMs alternately deposited with PDADMAC of M_w = 9000 g/mol, which is due to the smaller coil size of the PDADMAC, preventing thicker films.

IR Dichroism. The orientation of the α-helical PLG rods in the multilayer phase was checked by ATR-FTIR dichroism measurements. The p- and s-polarized ATR-FTIR spectra of the PEM containing four consecutively adsorbed layers (PEM-4) of PDADMAC/PLG are shown in Figure 7, where the PEM-4 in contact with water at pH = 3 on the untexturized substrate is shown in Figure 7a and the respective PEM-4 on the texturized substrate is shown in Figure 7b.

Qualitatively, the dichroic ratios ($R = A_p/A_s$) of amide I and II are different for the texturized and untexturized case, suggesting a certain polarization of the amide bands caused by anisotropic assembly of the α-helical PLG rods. Quantitative orientation analysis applied here is based on eqs 5−8, which were introduced in the theory section. The experimental dichroic ratios R_y^{ATR} and the calculated order parameter S are listed in Table 1.

TABLE 1: Experimental Dichroic Ratios R_y^{ATR} and Calculated Order Parameters S of the PEM-4 of PDADMAC/PLG on the Untexturized and Texturized Si−IRE in Contact with Water (wet) at pH = 3 (peak heights were evaluated)

	untexturized/wet		texturized/wet	
	amide I[a]	amide II	amide I	amide II
R_y^{ATR} (±0.05)	1.15	2.13	0.84	2.48
S (±0.10)	0.24	0.27	0.51	0.38
γ (±5°)	44°	45°	35°	40°

[a] The amide I band (peak, area) might be slightly influenced by the uncompensated δ(OH)-band of water.

TABLE 2: Order Parameters S and Cone Distribution Angles γ of PEMs Consisting of α-Helical PLG (70000 g/mol) Consecutively Adsorbed with Oppositely Charged PDADMAC (M_w = 250000, 9000 g/mol) or PVS, Respectively (The mean S value based on amide I and amide II dichroic ratio was taken)

PEM sample	S	γ (deg)
PDA-250000/PLG-70000, c = 0.01 M, wet	0.19	47
PDA-250000/PLG-70000, c = 0.005 M, wet	0.19	47
PDA-250000/PLG-70000, c = 0.001 M, wet	0.30	43
PDA-9000/PLG-70000, c = 0.001 M, wet	0.45	37

For the untexturized case the R_y^{ATR} values of amide I and II of the PLG were 1.15 and 2.13, respectively, from which a minor order parameter of $S \approx 0.2$ could be calculated. This value does not suggest a significant unidirectional alignment of the PLG rods in the PEM; however, a certain minor alignment did also occur in that sample. In contrast, for the texturized substrate R_y^{ATR} values of 0.84 and 2.38 were observed for the amide I and II bands, respectively. From this S values of 0.51 and 0.38 could be calculated, respectively. Hence, with an averaged order parameter around S = 0.45, a significant unidirectional orientation of the PLG α-helices along the texturized grooves could be concluded.

Influence of the Concentration and the Molecular Weight of PDADMAC. In Table 1 it was shown that the surface texture of the substrate has a very significant influence on the orientation of the PLG embedded in the PEM. Additionally, as molecular parameters, the influence of the PLG concentration and of the PDADMAC molecular weight was studied. In Table 2 the order parameters for three different concentrations at constant M_w = 250000 g/mol and for two molecular weights of PDADMAC at a constant concentration of 0.001 M of the PEM consisting of PDADMAC/PLG are shown.

Significantly, decreasing the concentration from c = 0.01, 0.005, to 0.001 M of the PDADMAC and the PLG solution led

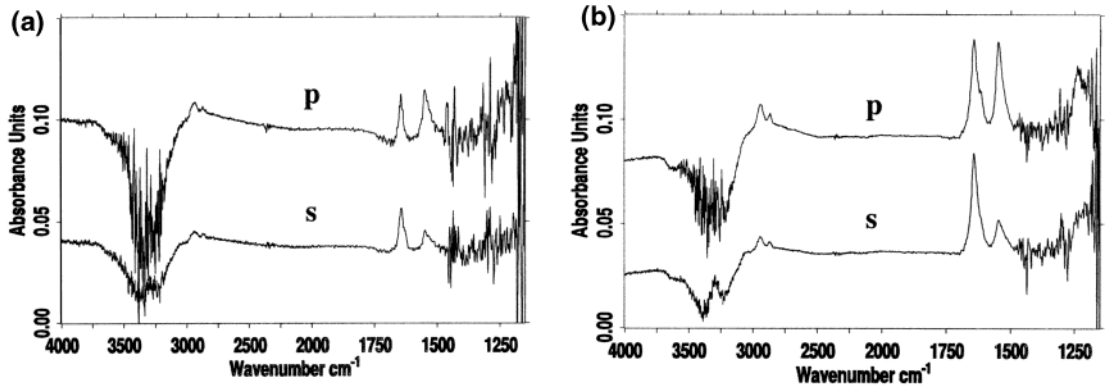

Figure 8. (a) p- and s-polarized ATR-FTIR spectra of a PEM-5 of α-PLL (M_w = 200000 g/mol) and PVS at pH = 11 (both PEL solutions) on the untexturized surface in contact with water (wet state). (b) p- and s-polarized ATR-FTIR spectra of a PEM-5 of α-PLL (M_w = 200000 g/mol) and PVS at pH = 11 (both PEL solutions) on the texturized surface in contact with water (wet state).

to a slight increase of the order parameter from $S = 0.19$ to 0.30. Possibly, the amount of adsorbed PDADMAC scales with the concentration shown in Figure 6b, and therefore, the PLG rods in the grooves were disturbed in their alignment by the PDADMAC coils.

Furthermore, the lower molecular weight PDADMAC (9000 g/mol) caused a higher order parameter of the PLG ($S = 0.45$) in comparison to the PDADMAC with the higher molecular weight (250000 g/mol) ($S = 0.30$). Obviously, the shorter PDADMAC chains revealed less perturbation for the alignment of the α-helical PLG rods in the silicon grooves.

α-PLL/Polyanion at pH = 11. Analogously to the PEM-4 of PDADMAC/PLG at pH = 3, the PEM-5 of PLL/PVS was deposited at pH = 11 onto texturized and untexturized Si−IREs. At that pH PLL adopts the α-helical conformation. Again, dichroic ATR-FTIR spectroscopy was applied to characterize the orientation state of the α-helical PLL rods alternately adsorbed with PVS by the order parameter *S*. In Figure 8 ATR-FTIR spectra measured by parallel (p) and vertical (s) polarized IR light of PEM-PLL/PVS-5 for the untexturized (a) and texturized case (b) are shown. From Figure 8a dichroic ratios $R_y^{ATR} = A_p/A_s = 1.12$ for the amide I and $R_y^{ATR} = 2.20$ for the amide II could be observed for the multilayer embedded PLL on the untexturized substrate. It should be noted that in this case we could not achieve a proper compensation of the water bands ν(OH) around 3400 cm^{-1} and δ(OH) around 1640 cm^{-1}, which might influence the intensity of the amide I band. Nevertheless, even with proper compensation the amide I band of the p-spectrum should be even higher compared to the s-spectrum, which would further increase the R_y^{ATR} and lower the *S* value. Thus, for the untexturized case, we obtained lower value order parameters of $S = 0.26-0.29$ for PLL. However, significantly, for the texturized substrate, dichroic ratios of $R_y^{ATR} < 1$ for the amide I band and $R_y^{ATR} \gg 1$ for the amide II band were obtained from the polarized spectra shown in Figure 8b.

From this, qualitatively, a polarization of the PLL amide bands could be observed and the calculated order parameters $S = 0.41-0.54$ were significantly higher compared to the untexturized case, which is summarized in Table 3.

Hence, a significant degree of unidirectional orientation for the multilayer embedded stiff PLL-α-helices along the texturization direction could be concluded. For the untexturized case, principally a minor degree of unidirectional order can be stated; however, since the *S* values were not equal to 0, a certain alignment prevailed even without texturization, which was also observed for the PEM of PDADMAC/PLG.

TABLE 3: Experimental Dichroic Ratios R_y^{ATR} and Calculated Order Parameters *S* of the PEM-5 of PLL/PVS on the Untexturized and Texturized Si−IRE in Contact with Water (wet) at pH = 11 (peak heights were evaluated)

	untexturized/w et		texturized/wet	
	amide I[a]	amide II	amide I[a]	amide II
R_y^{ATR} (±0.05)	1.12	2.20	0.94	3.11
S (±0.10)	0.26	0.29	0.41	0.54
γ (±5°)	45°	43°	39°	34°

[a] The amide I band (peak, area) might be slightly influenced by the uncompensated δ(OH)-band of water.

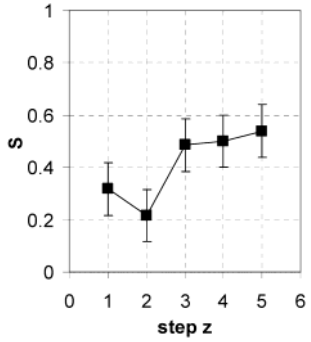

Figure 9. Order parameter *S* of α-helical PLL (M_w = 200000 g/mol) in PEMs of PLL/PVS based on the amide II band plotted with dependence on the adsorption step *z*. PLL and PVS solutions at pH = 11 were used.

Influence of the Layer Number. To check for the influence of the number of PEL layers on the unidirectional alignment, the individual order parameters for the PEM-1 to PEM-5 were determined based on the dichroic ratios. In Figure 9 the order parameter *S* of PLL based on the amide II band is plotted against the layer number.

Interestingly, the first PLL layer resulted in a minor order parameter ($S = 0.30$) compared to the last PLL layer ($S = 0.54$). With the exception of the second step, *S* increased in dependence of the layer number, presumably adopting a constant value from the 5th layer on between $S = 0.5-0.6$. This shows that the more PLL rods are adsorbed within the nanogrooves, the better they are aligned. This might be interpreted by the decrease in available space, which diminishes the PLL mobility within the surface groove. This progressive confinement might be also performed by the polyanions which complex the cationic PLL rods functioning as an electrostatic glue (see model below).

TABLE 4: Influence of Layer Number, Sample State (wet/dry), M_w of PLL, and Polyanion Type on the Order Parameter S and Cone Opening Angle γ of Multilayered PLL on Texturized Si−IREs (here the α-helical conformation was induced by $NaClO_4$ (c = 0.01 M))

PEM sample	S	γ (deg)
PLL-20000/PVS, PEM-10, wet	0.15	49
PLL-200000/PVS, PEM-10, wet	0.59	32
PLL-20000/PVS, PEM-5, wet	0.00	55
PLL-200000/PVS, PEM-5, wet	0.75	24
PLL-300000/PVS, PEM-5, wet	0.82	20
PLL-200000/PAC, PEM-5, wet	0.70	27
PLL-200000/PMA-MS, PEM-10, wet	0.47	37
PLL-200000/PVS, PEM-10, dry	0.49	36
PLL-200000/PMA-MS, PEM-10, dry	0.46	37

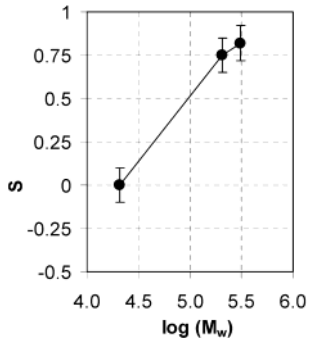

Figure 10. Order parameter S of α-helical PLL in PEMs of PLL/PVS with dependence on the M_w of PLL. PLL and PVS solutions in the presence of 1 M $NaClO_4$ were used.

PLL/polyanion in the Presence of 1 M $NaClO_4$

Dichroic data on PEMs containing α-helical PLL, whose conformation was kept at 1 M $NaClO_4$, and various polyanions were published recently.[10] In addition to that work, various factors influencing unidirectional orientation were studied, which were the molecular weight (M_w) of PLL, the polyanion type (PAC, PMA-MS, PVS), and the wet or dry state of the sample. The results are displayed in Table 4.

The molecular weight (M_w) of PLL has the most significant influence on its orientation in the surface grooves: PEM-5 of PLL of M_w = 20000 g/mol (PLL-20000) combined with PVS showed an order parameter of $S = 0.0$, whereas PEM-5 of PLL with M_w = 200000 and 300000 g/mol (PLL-200000, PLL-300000) combined with PVS high values of $S = 0.75$ and 0.82, respectively were found. Obviously, the PLL-20000, for which an ideal contour length of ≈15 nm was approximated, due to the height of 1.5 nm per helix turn, is too short to orient within the $L \approx 50-70$ nm wide grooves. PLL-200000 and PLL-300000 with contour lengths of approximately $L \approx 150$ and 225 nm are significantly longer with respect to the groove width. In Figure 10 the order parameter of PLL is plotted against the logarithm of M_w. Obviously, the α-helical rods intermolecularly complexed with the polyanion self-assembled and oriented *in-plane* with respect to the surface groove direction.

The complexing polyanions PMA-MS, PAC, and PVS used had only a small influence on orientation. The PLL order parameter in PEM-5 composed of PLL/PAC was $S = 0.70$ in comparison to $S = 0.75$ for PLL/PVS, and that in PEM-10 composed of PLL/PMA-MS was $S = 0.47$ compared to $S = 0.59$ for PLL/PVS. Hence, there was a slight order enhancement, if any, within the PEMs consisting of the sulfate containing strongly charged polyanion PVS compared to the carboxyl containing weaker charged PAC or PMA-MS.

Drying the oriented PEM caused a minor decrease of unidirectional order from $S = 0.59$ to 0.49 for the PEM-10 of PLL/PVS and practically no decrease (wet, $S = 0.47$; dry, 0.46) for the PEM-10 of PLL/PMA-MS. Therefore, both rinsing with water and drying PLL preserved its α-helical conformation, which is not shown here, proven by ATR−IR-spectra.

Discussion

It is not fully understood which interaction forces may play a role in causing the α-helical polypeptide rods to assemble predominantly within the surface grooves and not to span across the surface grooves. Possibly, in the scratched silicon grooves there is a higher population of reactive geminal Si−OH groups, causing more surface contacts with the α-helical polypeptides, especially PLL. Also, capillary forces between the stiff extended polypeptide rods and the equally dimensioned surface groove may occur. Considering charged α-PLL rods in 'half pipes', it also evident that the rods can interact not only with the oppositely charged surface of the bottom but also with the side walls within an open half cylinder and therefore have more surface contacts compared to the planar surface. The same holds for α-PLG if the negatively charged surface is overcompensated by positive surface charge through PDADMAC adsorption in the first step. However, it was shown that in that case there was a significant influence on the molecular weight of PDADMAC, so that the grooves were filled too much using PDADMAC-250000 in contrast to PDADMAC-9000.

Recently, a theoretical study of Park[34] was published concerning the orientation behavior of stiff polyelectrolytes in microchannels with like charged channel wall. Two cases were distinguished: (i) under conditions of maximum electrostatic repulsion (low ionic strength, high surface charge, i.e., large Debye length), a perpendicular orientation of the rods was obtained; (ii) under conditions of minimum electrostatic interaction (small Debye length), a parallel orientation of the rods was obtained, since steric and entropic factors ('entropic surface exclusion') prevail, to minimize the excluded volume. Since the PLL rods were formed at high ionic strength (1 M $NaClO_4$), case ii would be valid for our system, whose result is qualitatively consistent with our experimental findings of parallel orientation in the 'half channels'. Even for the PEMs of PLL/PVS and PLG/PDADMAC the PLL rods complexed with polyanions should be only weakly charged, and hence, these systems could be also explained by case ii.

Model Proposition. As it is shown in Figure 11a, the order parameter S can be illustrated by the double cone model, whereby more or less unidirectionally aligned α-helical rods are forming a bundle within the silicon surface grooves. These rods can be shifted without changing the angles between them, so that their centers of gravity are all in one point. This reduces the rod arrangement to a double cone, and its opening angle γ is a measure of their more or less uniaxial alignment: small γ values are due to high order, and large γ values are due to low order. Using eq 8 it is possible to determine γ from S, which is given in Tables 1−4 for the PEMs studied. On the basis of these γ values, an arrangement of the rods is suggested in Figure 11b where the stiff α-helical polypeptides are linked together by coils of oppositely charged polyelectrolytes.

Therefore, the α-helical conformation or the stiffness of the polypeptides is stabilized either by pH = 3 in the case of PLG and by pH = 11 in the case of PLL or by specific interaction of bulky low molecular counterions such as ClO_4^- in the case of PLL. The latter stabilization is claimed to be caused by specific insertion of the ClO_4^- anions within the ammonium groups of PLL,[35] whereas the pH stabilization acts as a neutralization of the side chains which causes the formation of

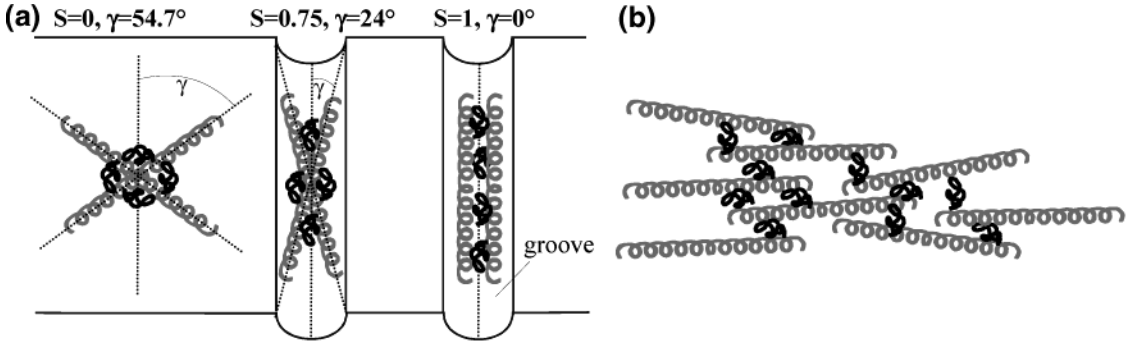

Figure 11. (a) Double cone model of more or less aligned α-helices in surface grooves of the Si−IRE. The opening angle γ scales with the order parameter *S*. (b) Model proposition of the PEM phase consisting of stiff α-helical polypeptides and their coiled oppositely charged polyelectrolyte partner: Coiling of the non-peptidic component by salt ('Screening') and α-helix induction of the polypeptide by specific interaction.

the α-helix as pointed out before. On the other hand, the oppositely charged nonpeptidic polyelectrolytes are expected to be in a more coiled conformation. This is surely the case for the system PLL/PVS/$NaClO_4$: due to the high ionic strength (1 M $NaClO_4$), the PVS is coiled due to the classical charge shielding effect of low mineral salt. For the system PLL/PVS at pH = 11, we also assume a certain coiling of the PVS, since at this pH a NaOH concentration of 10^{-3} M is present. The same concentration of HCl (10^{-3} M) should be present for the system PLG/PDADMAC at pH = 3, also inducing a coiling of the PDADMAC. Thus, by both $NaClO_4$ or pH we cause, on one hand, a specific helicalization of the polypeptide and, on the other hand, the classical salt-induced coiling of the nonpeptidic PEL component. However, despite this intramolecular charge shielding, there is still intermolecular attraction between the oppositely charged polypeptide and the strong polyelectrolyte (PLL/PVS, PLG/PDADMAC), which might be caused by additional nonelectrostatic (e.g., hydrophobic, van der Waals) interaction.

These results show that consecutively adsorbed stiff polyelectrolytes do form anisotropic PEM phases in contrast to flexible ones, in which the unordered and somewhat 'fuzzy phase' is claimed to be composed of Gaussian coils.[2,4,6,7] The PEMs shown here consisting of α-helical polypeptides are exceptions from these classical PEMs. Anisotropic PEMs were already shown by Laschewsky, who reported lamellar structures in PEMs composed of lyotropic ionenes and strong polyanions,[8] and by Kleinfeld and Ferguson, who studied PEMs of polycations and exfoliated sheets of Laponite.[9]

The results also show that by using the multilayer concept and texturized substrates α-helical PLL could be both immobilized and oriented in thin films. Furthermore, these surfaces can be used to generate and study specific biomimetic or biorecognitive properties of PEMs.[36] In that framework we extend our findings on electrostatic interaction between proteins and the outermost layer of PEMs[11,37−39] to nonelectrostatic interactions due to recognition on the polypeptide conformation level.

Summary

Anisotropic polyelectrolyte multilayers (PEM) were generated on texturized and untexturized Si substrates using stiff anionic and cationic α-helical polypeptides such as PLG and PLL and were characterized by dichroic ATR-FTIR spectroscopy.

The number of adsorbed layers, concentration, and molecular weight of the PEL components were found to be important parameters for the degree of unidirectional orientation of the multilayer embedded α-helical polypeptides within the parallel surface grooves.

For PEMs consisting of PDADMAC and α-PLG, an increase of order with decreasing PEL concentration was found. PDADMAC of M_w = 9000 g/mol caused higher unidirectional order of multilayered α-PLG within the surface grooves (50−70 nm wide) compared with PDADMAC of M_w = 250000 g/mol due lower steric perturbation of the assembling α-PLG rods.

For PEMs consisting of α-PLL and PVS (pH = 11), an increase of order with increasing adsorption steps was found. Significantly, in PEM-5 ($NaClO_4$), α-PLL of M_w = 200000 and 300000 g/mol ($S > 0.75$) showed higher parallel alignment within the surface grooves compared to α-PLL with M_w = 20000 g/mol ($S = 0$) due to the higher contour length and aspect ratio with respect to the groove width.

A nanoscopic model consisting of unidirectionally oriented α-helical polypeptide rods intermolecularly glued by oppositely charged coiled PELs was assumed.

Further studies will focus on the orientation of other synthetic PELs and will contribute to fundamental studies on the behavior of stiff polyelectrolytes in the confined space of surface textures.

Acknowledgment. We thank the Deutsche Forschungsgemeinschaft (DFG) for funding these studies within the Sonderforschungsbereich SFB 287 (TP-B5) and the Schwerpunktprogramm Polyelektrolyte SPP-1009 (MU-1524-1/1). We also thank Prof. H.-J. Adler (TU Dresden, SFB 287) for stimulating discussions.

References and Notes

(1) Decher, G.; Hong, J. D.; Schmitt, J. *Thin Solid Films* **1992**, *210/211*, 831.
(2) Decher, G. *Science* **1997**, 1232.
(3) Lvov, Y.; Haas, H.; Decher, G.; Möhwald, H. *Langmuir* **1993**, *9*, 481.
(4) Arys, X.; Jonas, A. M.; Laguitton, B.; Lasschewsky, A.; Legras, R.; Wischerhoff, E. *Thin Solid Films* **1998**, *327−329*, 734.
(5) Schmitt, J.; Grünewald, T.; Kjaer, K.; Pershan, P.; Decher, G.; Lösche, M. *Macromolecules* **1993**, *26*, 7085.
(6) Borue, V. Y.; Erukhimovich, I. Y. *Macromolecules* **1990**, *23*, 3625.
(7) Castelnovo, M.; Joanny, J. F. *Langmuir* **2000**, *16* (19), 7524.
(8) Arys, X.; Laschewsky, A.; Jonas, A. M. *Macromolecules* **2001**, *34*, 3318.
(9) Kleinfeld, E. R.; Ferguson, G. S. *Science* **1994**, *265*, 370.
(10) Müller, M. *Biomacromolecules* **2001**, *2*, 262.
(11) Müller, M.; Rieser, T.; Lunkwitz, K.; Berwald, S.; Meier-Haack, J.; Jehnichen, D. *Macromol. Rapid Commun.* **1998**, *19* (7), 333.
(12) Fringeli, U. P. In *Encyclopedia of Spectroscopy and Spectrometry*; Lindon, J. C., Tranter, G. E., Holmes, J. L., Eds.; Academic Press: New York, 2000.
(13) Fringeli, U. P. *Z. Naturforsch.* **1977**, *32c*, 20.
(14) Larsson, M. L.; Holmgren, A.; Forsling, W. *Langmuir* **2000**, *16*, 8129.
(15) Singh, P. K.; Adler, J. J.; Rabinovich, Y. I.; Moudgil, B. M. *Langmuir* **2001**, *17*, 468.

(16) Fringeli, U. P.; Schadt, M.; Rihak, P.; Hs. Günthard, H. *Z. Naturforsch*. **1976**, *31a*, 1098.
(17) Fringeli, U. P.; Hs. Günthard, H. In *Membrane Spectroscopy*; Grell, E., Ed.; Springer: Berlin, 1981; p 270.
(18) Zbinden, R. *IR−Spectroscopy of High Polymers*; Academic Press: New York, 1964.
(19) Hermans, P. H.; Platzeck, P. *Kolloid-Z.* **1939**, *88*, 68.
(20) Jasse, B.; Koenig, J. L. *J. Macromol. Sci. Rev. Macromol. Chem. C* **1979**, *17*, 61.
(21) Miyazawa, T. *J. Chem. Phys.* **1960**, *32*, 1647.
(22) Krimm, S. *J. Mol. Biol*. **1962**, *4*, 528.
(23) Marsh, D.; Müller, M.; Schmitt, F. J. *Biophys. J.* **2000**, *78*, 2499.
(24) Wegner, G. *Mol. Cryst. Liq. Cryst.* **1993**, *235*, 1.
(25) Schmitt, F. J.; Müller, M. *Thin Solid Films* **1997**, *310* (1−2), 138−147.
(26) Greenfield, N.; Fasman, G. D. *Biochemistry* **1969**, *8* (10), 4108−4116.
(27) Cassim, J. Y.; Yang, J. T. *Biopolymers* **1970**, *9*, 1475.
(28) Müller, M. ETH Diss. No 10422; Eidgenössische Technische Hochschule, Zürich, 1993.
(29) Müller, M.; Buchet, R.; Fringeli, U. P. *J. Phys. Chem.* **1996**, *100* (25), 10810.
(30) Ebert, C.; Ebert, G.; Werner, W. *Kolloid Z. Z. Polymere* **1973**, *251*, 504.
(31) Nevskaya, N. A.; Chirgadze, Y. N. *Biopolymers* **1976**, *15*, 637.
(32) Müller, M. In *Handbook of Polyelectrolytes and Their Applications*; Tripathy, S. K., Kumar, J., Nalwa, H. S., Eds.; American Scientific Publishers (ASP): 2002; Vol. 1, pp 293−312.
(33) Visual inspection of a molecular model of α-helical polypeptides.
(34) Chun, M.-S.; Kim, S. I.; Park, O. O. *Colloids Surf. A* **2002**, *205*, 261.
(35) Ebert, G.; Kim, Y.-H. *Prog. Colloid Polym. Sci*. **1983**, *68*, 113.
(36) Müller, M.; Kessler, B. Manuscript in preparation.
(37) Müller, M.; Rieser, T.; Lunkwitz, K.; Meier Haack, J. *Macromol. Rapid Commun*. **1999**, *20* (12), 607−611.
(38) Müller, M.; Briššová, M.; Rieser, T.; Powers, A. C.; Lunkwitz, K. *Mater. Sci. & Eng. C* **1999**, *8−9*, 163−169.
(39) Müller, M.; Rieser, T.; Dubin, P.; Lunkwitz, K. *Macromol. Rapid Commun*. **2001**, *22* (6), 390−395.